High-mass star-forming regions in the Large Magellanic Cloud

Peter Schilke[1], Roya Hamedani Golshan[1], Marta Sewiło[2], Álvaro Sánchez-Monge[1,3]

[1]I. Physics Institute, University of Cologne, Germany
[2]Department of Astronomy, University of Maryland, STSC, Nasa Goddard Space Flight Center, USA
[3]Institute of Space Sciences (ICE-CSIC), Barcelona, Spain

Star Formation in the LMC

While in very massive and merging starburst galaxies in the Early Universe accelerated star formation activity quickly formed heavy elements and resulted in a near solar metallicity in these objects, this was not the case for the bulk of normal galaxies at that time.

Hence, star formation in those objects occurred under low-metallicity conditions (Pei et al., ApJ 522, 604, 1999; Mannucci et al., MNRAS 408, 2115, 2010). Since high spatial resolution observations of the scales considered here (≤ 5 pc) are not possible at high redshifts, we have to revert to local templates that approximate these conditions.

One such local template are the Magellanic Clouds, dwarf companions of the Milky Way with lower metallicities: $Z \approx 0.3 - 0.5\ Z_\odot$ for the LMC (Choudhury et al., MNRAS 455, 1855, 2016), and $Z \approx 0.1 - 0.2 Z_\odot$ for the SMC (Choudhury et al., MNRAS 475, 4279, 2018). This corresponds to typical metallicities of galaxies at redshifts in the range 2.5 to 3 (Mannucci et al. 2010).

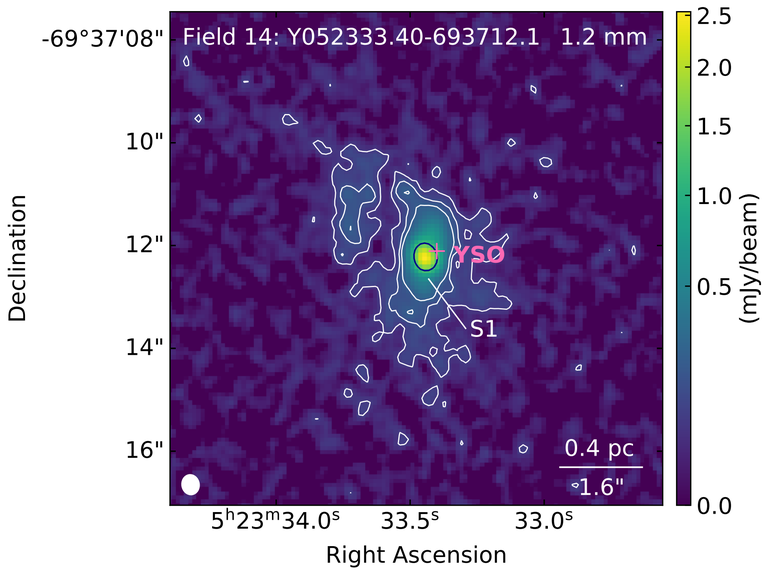

Figure 2: ALMA continuum map of Y052333.40-693712.1, one of our 20 sources.

Our Data

Our aim was to characterize the chemical composition of sources in the LMC (Fig. 1) to see if the different environmental conditions also affect very deeply embedded sources. We therefore selected 20 YSOs, without ice features, without fine structure lines (Seale et al. 2009, ApJ, 699, 150), located away from massive star-forming sites and with Herschel counterparts (Seale et al. 2014, AJ, 148, 124) to maximize the chance of selecting the evolutionary stage of hot cores and not earlier or later stages. These sources were observed with ALMA in project 2017.1.00696.S. The observations were carried out as single pointing lasting 19.3 minutes on each field with 0.4″ angular resolution and 5.4″ maximum recoverable angular scale. The spectral setup covered four windows, at 241.6, 244.6, 257.6, and 259.5 GHz.

Data Analysis

In the 20 fields, 65 compact continuum sources were found, among them 31 with fluxes larger than 10 σ. Those we analyzed with XCLASS (Möller et al. 2017, A&A, 598, A7), using data mostly from VAMCD/CDMS (Endres et al. 2016, JMoSp, 327, 95). Methanol lines are ubiquitous in our sample, except toward two of the cores. Other molecular lines with high detection rate are CS, SO, SO_2, $H^{13}CO^+$, $H^{13}CN$, $HC^{15}N$, H_2CS and SiO. More complex molecules such as HDCO, HNCO, HC_3N, CH_3CN and high excitation transitions of SO and SO_2 isotopologues are detected only toward a small subset of the cores (see Fig. 3 for an example).

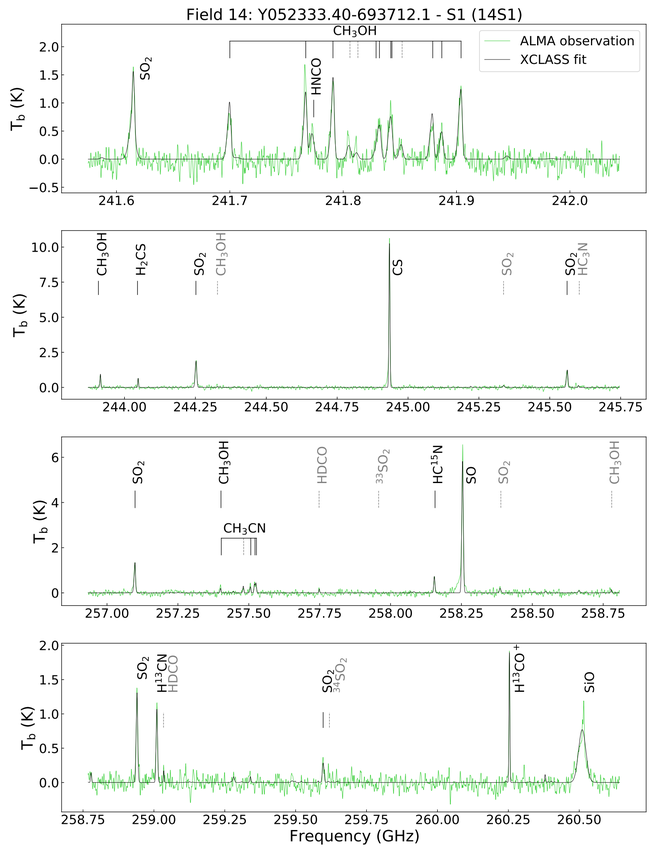

Figure 3: Observed spectra overlaid with the best fitted XCLASS model for our new hot core S1 in Fig. 2. Definite detection of rotational transitions is marked with a continuous black line, and tentative detection with a dotted gray line .

Temperatures

We fit the temperature for three molecular tracers SO_2, CH_3OH and CH_3CN, if they are reliably detected. In some cores, SO_2 and CH_3OH need more than one temperature component. For the rest of the molecules, we fix the temperature either to the the average value of SO_2 and CH_3OH or to CH_3CN, when that is available. In Fig. 4 one can see that the spread of temperatures is considerable, probably due to different molecules tracing different source structures.

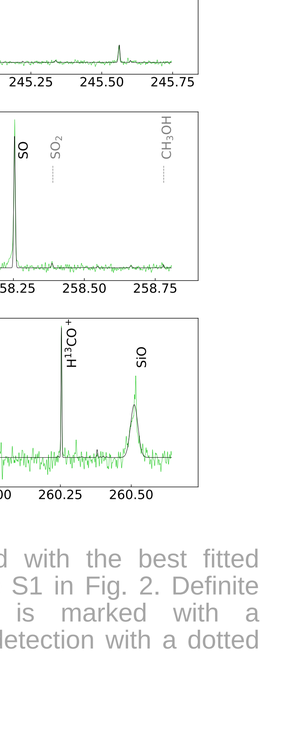

Figure 4: XCLASS fitted temperatures, ordered by core mass.

Figure 1: The color-composite image of the LMC combining the Hα (blue: Smith & MCELS Team 1998, PASA 15, 163), SAGE/IRAC 8 μm (green, Meixner et al. 2006, AJ, 132, 2268) and HERITAGE/SPIRE 350 μm (red, Meixner et al. 2013, AJ, 146, 62). The 20 ALMA fields are overlaid with the yellow circles sized 15 times the observed field of view.

Abundances

In Fig. 5 we show the abundances we obtained. This result confirms the previous detection of hot cores in ST16 YSO (Shimonishi et al. 2020, ApJ, 891, 164) and two hot cores in N105 (Sewiło et al. 2022, ApJ, 931, 102). In addition, we present a new hot core detection in field Y0523333.40-693712.1 (Fig. 2 and 3). We note that there are uncertainties associated with these abundances, due to the approximation of one or two component LTE fitting, that does not take the source complexities into account, and also uncertainties of opacities for species with few lines.

Our next steps will involve quantifying these uncertainies, and comparing with both Galactic abundances and chemical models.

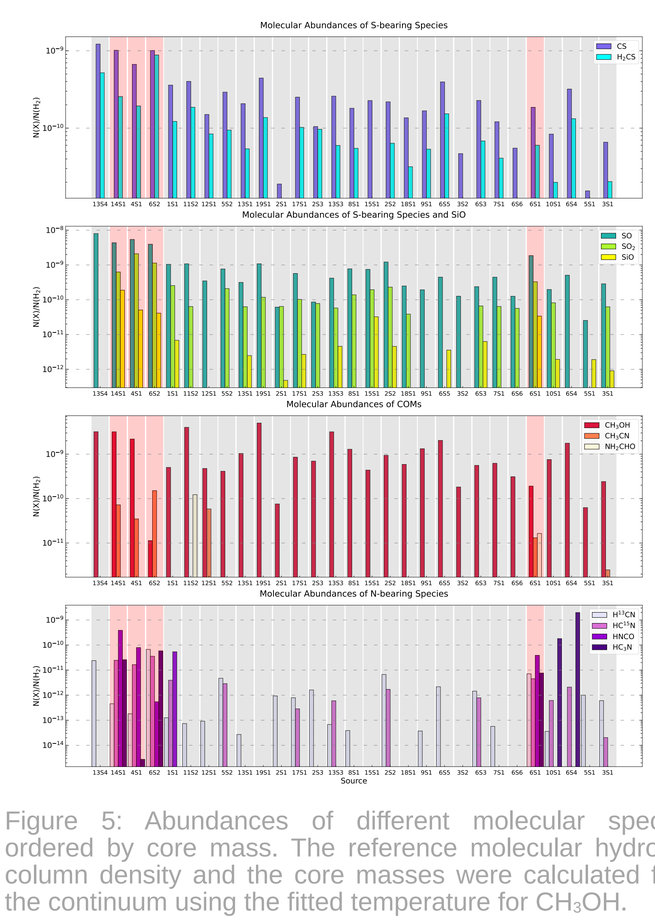

Figure 5: Abundances of different molecular species, ordered by core mass. The reference molecular hydrogen column density and the core masses were calculated from the continuum using the fitted temperature for CH_3OH.

RHG and PS acknowledge funding by the Deutsche Forschungsgemeinschaft (DFG, German Science Foundation) Project SCHI 561/1-1.